Chapter X

Environmental effects on photoluminescence of single-walled carbon nanotubes

Yutaka Ohno, Shigeo Maruyama*, and Takashi Mizutani
Department of Quantum Engineering, Nagoya University
**Department of Mechanical Engineering, The University of Tokyo*
Japan

1. Introduction

Spectroscopy is a powerful technique to characterize single-walled carbon nanotubes (SWNTs). In particular, photoluminescence (PL) and the excitation spectroscopies have made a great advance in understanding the energy states and transition processes of excitons in SWNTs. The PL spectroscopy also has a potential to assign the chiral index (n,m) of a SWNT and to evaluate the abundance of (n,m) in bulk SWNTs. (Bachilo et al., 2002, Miyauchi et al., 2004). In order to establish the PL spectroscopy as a reliable standard technique to characterize SWNTs, it is necessary to understand not only the intrinsic physics of excitons, but also the effect of extrinsic factors, so-called *environmental effects*. (Fantini et al., 2004) The optical property of SWNTs is modified sensitively by the environmental condition around the SWNT, since excitons exist on the surface of the SWNT. In this chapter, we focus on the environmental effects on the optical properties of SWNTs. After fundamental physics of the optical transition and PL spectroscopy in SWNTs, various types of environmental effects are discussed with the practical examples.

2. Optical transition and photoluminescence in SWNTs

2.1 Density of states and optical transition

In a SWNT, electrons are confined on the surface of the SWNT, and the wave vectors along the circumference are quantized by the periodic boundary condition. The carriers are free to move along the direction of the SWNT axis. Therefore, the SWNT has a one-dimensional electron system, where the density of states is characterized by the sharp peaks originating from van Hove singularity as shown in Fig. 1(a). (Saito et al., 1998)

The optical transition in a SWNT occurs dominantly between two subbands at van Hove singularities. Because of the one-dimensional structure, the optical transition depends on the polarization of the incident light. If the incident light is polarized linearly parallel to the SWNT axis, the strong optical transition occurs. In this case, the optical transitions between two subbands of a conduction band and of a valence band with a same quantum number are allowed by the selection rule. For example, the transitions such as from C1 to V1 and

from V2 to C2 are allowed transitions as shown in the figure. In the case of the light polarized perpendicular to the SWNT axis, on the other hand, the optical transition is strongly suppressed by the depolarization effect, in which the induced charges cancel the electric field of the light in the SWNT. (Duesberg et al., 2000)
The energy of the optical transition is given by the difference in energy of the two subbands, in the range of the single particle approximation. In practice, it is modified by many body effects as shown in Fig. 1(b). (Ando, 2005) The single particle bandgap E_{ii}^{gr} is renormalized by the self-energy of an electron due to a repulsive interaction between electrons. For an optical transition, the exciton effect should be taken into account, that is, the optical transition energy is decreased by the binding energy of the attractive Coulomb interaction between an electron and a hole. In the case of SWNTs, since the exciton binding energy is as large as a few hundred meV, the exciton scheme is more suitable than the single particle scheme. (Wang et al., 2005) Consequently, the optical transition energy E_{ii} between the i-th valence band and i-th conduction band (i = 1, 2, 3, ...) is given by

$$E_{ii} = E_{ii}^{gr} + E_{ii}^{ee} + E_{ii}^{eh}, \quad (1)$$

where E_{ii}^{ee} is the energy of repulsive interaction between electrons, and E_{ii}^{eh} (< 0) is the binding energy of an exciton. Note that every term is perturbed by the environment around the SWNT as described later.

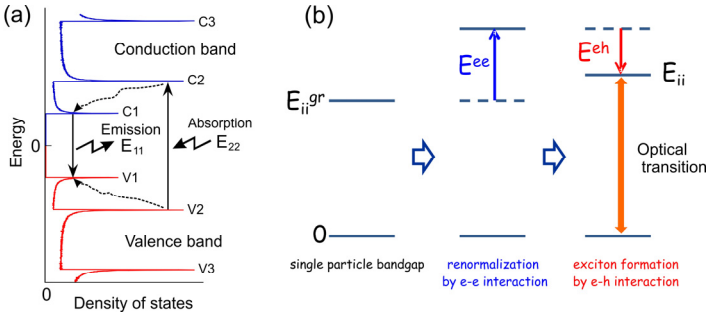

Figure 1 (a) The density of states of a semiconducting SWNT, and optical transition processes in the single particle scheme. (b) The energy diagram of an exciton state, showing optical transition energy in the exciton scheme.

2.2 Photoluminescence spectroscopy

Since the optical transition energy E_{ii} is dependent on the (n,m), (n,m) of SWNTs can be assigned by spectroscopic techniques such as Raman scattering spectroscopy (Kataura et al., 1999) and PL spectroscopy (Bachilo et al., 2002) In the case of PL spectroscopy of a semiconducting SWNT, the E_{22} state is resonantly excited by incident light to generate excitons as shown in Fig. 1(a). (O'Connell et al., 2002) The excitons relax via phonons to the E_{11} state, where radiative recombination occurs. Figure 2(a) shows the PL spectra of SWNTs measured for various excitation wavelengths. This measurement is called the PL mapping

measurement. Each peak comes from a different (*n*,*m*) specie. From the relative intensity of each peak, the abundance of each (*n*,*m*) specie can be evaluated. It should be note that the quantum efficiency for light absorption and emission depends on the diameter and chirality of SWNTs. (Oyama et al., 2006) In order to make accurate the evaluation of (*n*,*m*) abundance, a collection for (*n*,*m*) dependence of the quantum efficiency is necessary (Okazaki et al., 2006).

Figure 2(b) shows the E_{22}-E_{11} plot for various (*n*,*m*) species, which are derived from the PL map of Fig. 2(a). The points connected by a solid line belong to the family of SWNTs, which has a same number of $2n+m$. (Saito et al., 1998) The family pattern can be seen to be separated into two groups, depending on the value of ($2n+m$ mod 3). In this chapter, we define these two groups as Type-I if ($2n+m$ mod 3) = 1, and Type-II if ($2n+m$ mod 3) = 2. When a graphite layer is rolled up to form a SWNT, the quantized energies of the subbands primarily depend on the diameter of a SWNT. In addition, they are also dependent on the direction to be quantized, namely the chiral angle, since the equi-energy contours of graphite are warped to be a triangular shape around the *K* point, so-called the trigonal warping effect. (Saito et al., 2000). This is the main reason for the appearance of the family pattern in the plot of optical transition energies.

The family pattern is technically important for the analysis of PL spectra. Even though the optical transition energy of a SWNT varies more than 100 meV, depending on the methods to prepare the sample and on the environment, the identification of the family pattern allows us to assign easily the chirality (*n*,*m*) of SWNTs.

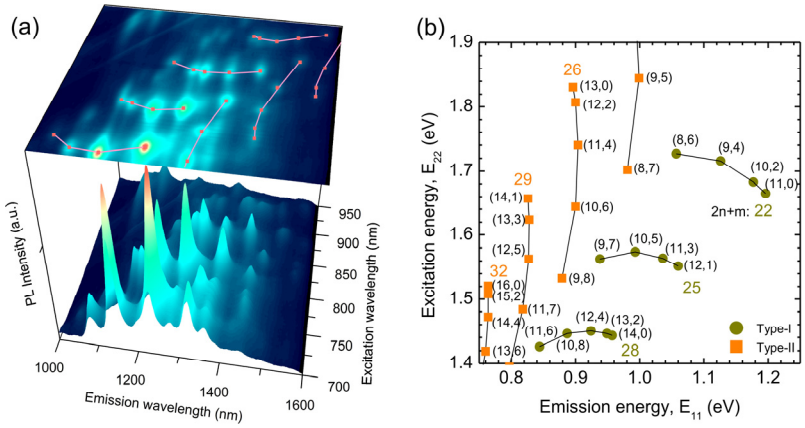

Figure 2 (a) PL spectra of SWNTs measured for various excitation wavelengths (PL map). (b) E_{22}-E_{11} plot. The solid lines connect a family of SWNTs with a same value of $2n+m$.

2.3 Relaxation process

In the PL processes, the excitons excited to the E_{22} state relaxe to the lowest state E_{11} via phonons in a short time as ~ 0.1 ps, since the optical phonon energy is as large as 0.2 eV (Ichida et al., 2002, Ostojic et al., 2004) Then, the excitons relax to the ground state via

radiative recombination or non-radiative recombination. The radiative recombination lifetime is expected to be in the magnitude of 1 ns. (Spataru et al., 2005) In contrast, the experimental results of the pump-probe measurements and the time-resolved PL measurements have shown a much shorter recombination lifetime as several ten ps. (Wang et al., 2004, Hagen et al., 2004, Ohno et al., 2006a, Hirori et a., 2006) The short recombination lifetime suggests that the dominant recombination process is non-radiative process. Recombination centers formed by defects and interface states may enhance non-radiative recombination. Non-radiative recombination is caused by multi-phonon relaxation process, which is enhanced if the exciton is localized. (Perebeinos et al., 2008) The luminescence quantum efficiency has been estimated experimentally to be several percent. (Lefebvre et al., 2006)

2.4 Sample preparation for photoluminescence

The soot of SWNTs generally consists of bundles of SWNTs formed by van der Waals interaction. In a bundle of SWNTs, the energy of photoexcited excitons is transferred to neighboring metallic SWNTs or SWMTs with a smaller bandgap, and then relax via phonons. In order to obtain luminescence from the SWNTs, it is necessary to debundle and individualize the bundle of SWNTs. O'Connell et al. have observed the first PL of SWNTs by wrapping SWNTs with a surfactant such as sodium-dodecyl-salfate (SDS) to form the micelles.(O'Connell et al., 2002) After dispersing the soot of SWNTs in the aqueous solution of SDS using ultrasonication, they obtained individualized SWNTs in the supernatant liquid of ultracentrifugation as shown in Fig. 3(a).

The other method to obtain individualized SWNTs is to grow SWNTs directly between pillars or on trenches formed on a Si substrate and a quartz substrate as shown in Fig. 3(b). (Lefebvre et al., 2004a, and Ohno et al., 2006b). The *free-standing* SWNTs bridging such a micro structure cause strong light emission, although the light emission is suppressed if the SWNT contacts with the substrate as will be described later. In the case of a free-standing SWNT, the PL signal is strong enough to observe an individual SWNT by microscopic PL technique.

For the study on environmental effects, the free-standing SWNTs grown between pillars or on trenches are suitable because the environmental conditions can be intentionally changed by exposing to a gas (Finnie et al., 2005, Chiashi et al., 2008) or immersing in a liquid (Ohno et al., 2007, Iwasaki et al., 2007).

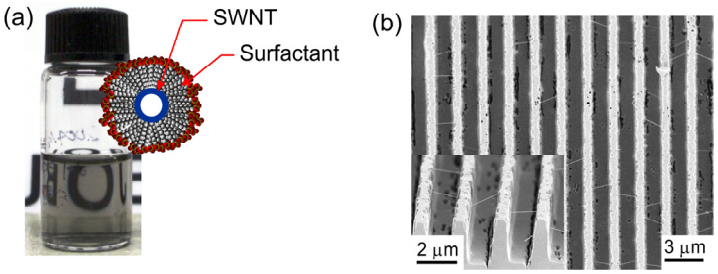

Figure 3 (a) Photograph of SWNTs dispersed in surfactant solution. (b) SEM image of free-standing SWNTs grown on the trenches formed on a quartz substrate.

3. Environmental effects

The environmental effect is one of the most important topics for the optical properties of SWNTs. (Moore et al., 2003, Chou et al., 2004, Fantini et al., 2004) It is known that the optical transition energy varies, depending on the kind of surfactants used to individualize SWNTs. Lefebvre et al. have also reported the optical transition energies of SWNTs bridging between micro-pillars show a blueshift as compared to the SDS-wrapped SWNTs. (Lefebvre et al., 2004b) Later work by Ohno et al. have shown that the energy differences depend on (*n*,*m*), especially on chiral angle and on type of SWNTs, type-I or type-II. (Ohno et al., 2006b) One of the causes of the variation in the optical transition energy is the dielectric screening of the many-body interactions between carriers. (Ando, 2005, Perebeinos et al., 2004) In addition to the dielectric screening effect, various environmental factors such as chemical interactions (Hertel et al., 2005, Finnie et al., 2005), and mechanical interactions (Arnold et al., 2004), should be considered. Comprehensive understanding of the environmental effects is necessary to understand the optical property of SWNTs. In this section, the effects of the dielectric screening, wrapping with surfactants, exposure to the air, doping of carriers, and contact with a substrate are discussed.

3.1 Dielectric screening effect

The variation of the optical transition energy caused by the environmental condition is primarily due to the dielectric screening effect, whereby the many-body Coulomb interactions between carriers are screened by the surrounding materials. As shown in Fig. 4, the electric force lines contributing to the Coulomb interactions pass through not only the inside of the SWNT but also the outside, where surrounding material screens the electric force lines, depending on the dielectric constant.

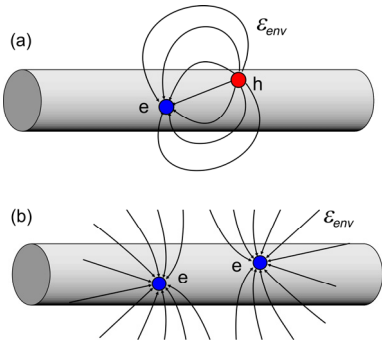

Figure 4 Schematics of electric force lines contributing to many body Coulomb interactions, (a) electron-hole attractive interaction, which forms an exciton, and (b)electron-electron repulsive interaction.

Ohno et al. have studied the dielectric screening effect in detail by immersing the SWNTs grown on trenches (Fig. 3(b)) in various organic solvents with dielectric constants from 1.9 to 37. (Footnote1) (Ohno et al., 2007, Iwasaki et al., 2007) Figure 5 shows the typical PL spectra measured in the ambient air, hexane (dielectric constant: 1.9), chloroform (4.8), and acetonitrile (37). The peaks show a red-shift and broadening with increasing the dielectric constant of liquids. As shown the E_{22}-E_{11} plots in the Fig. 6, both E_{11} and E_{22} show a red-shift with increasing the dielectric constant of liquids, with a small (n,m) dependence. The amounts of the red-shifts are 20~43 meV for E_{11} and 15~33 meV for E_{22}.

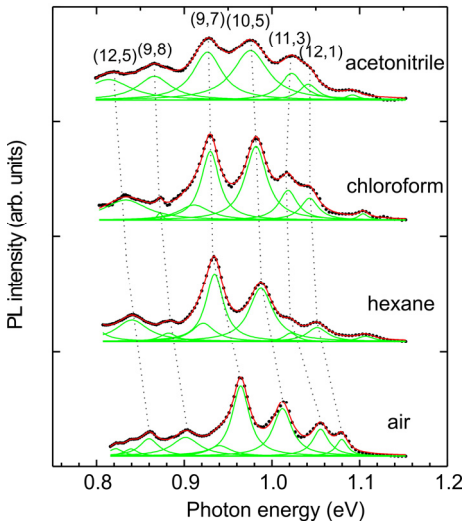

Figure 5 PL spectra in ambient air, hexane, chloroform, and acetonitrile.

With the dielectric constant increases, the energies of both electron-electron and electron-hole interactions are decreased. The reduction of the exciton binding energy causes a blue-shift in the optical transition energy because of the negative energy, whereas the reduction of the electron-electron repulsion energy causes a red-shift. The observation of red-shifts suggests that the variation of electron-electron repulsion energy is larger than that of exciton-binding energy. This is due to the fact that the repulsion energy is larger in magnitude than the exciton binding energy. (Ando, 2005, Spataru et al., 2005)
Figure 7 shows E_{11} and E_{22} of (8,6)-SWNTs as a function of dielectric constant of liquid. The energy shift is significant at the regime of low dielectric constant, and show a tendency to saturate at the dielectric constant of ~5. Empirically, the dependence of E_{ii} on the environmental dielectric constant ε_{env} is given by

$$E_{ii} = E_{ii}^{\infty} + A\varepsilon_{env}^{-\alpha}. \quad (2)$$

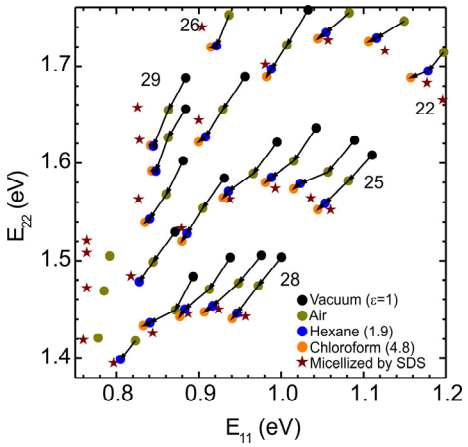

Figure 6 E_{22}-E_{11} plots of SWNTs grown on micro-trenches in various environment conditions, in vacuum (black dots), air (yellow green), hexane (blue), chloroform (orange), and aqueous solution of SDS (red stars).

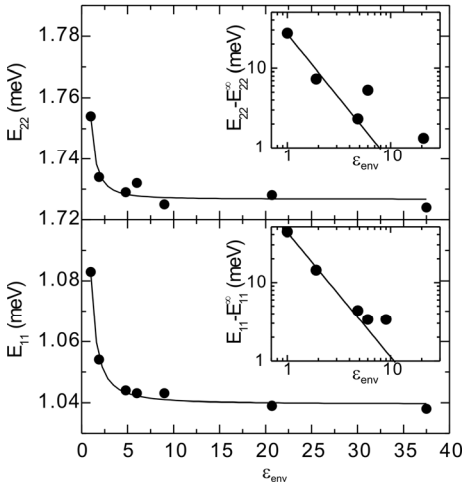

Figure 7 E_{11} and E_{22} of (8,6)-SWNTs as a function of the dielectric constant of liquid. The insets are the log-log plots.

The first term corresponds to a transition energy when ε_{env} is infinity, and consists of the single particle bandgap and the energies of the many body interactions which are determined by the electric force lines traveling only inside the SWNT. The second term shows the screening of Coulomb interactions including both exciton binding and electron-electron repulsive interactions, which are related to the electric force lines traveling outside the SWNT. A corresponds to the maximum energy variation. The solid curves in Fig. 6 are the fittings using Eq. (2). Here, A and α are 43 meV and 1.6 for E_{11}, and 27 meV and 1.8 for

E_{22}, respectively. Miyauchi et al. have also obtained a power-law-like dependence of the exciton transition energies on dielectric constant around SWNTs by the tight-binding calculation. (Miyauchi et al,. 2007)
The variation of E_{ii} due to the dielectric screening effect is also dependent on (n,m), especially, on the chiral angle, and the type (Type-I or Type-II). This can originate from the (n,m) dependence of effective mass of carriers. As descried before, effective mass depends on chiral angel because of the trigonal warping effect. (Jorio et al., 2005) The effective mass is one of the scaling parameters for exciton energy. (Perebeinos et al., 2004) Similarly, the repulsive energy of electron-electron interaction could be dependent on the effective mass.
It should be noted that the PL spectrum become broader in liquids with a large dielectric constant in addition to a red-shift as shown in Fig. 5. The full width at half maximum (FWHM) increased from 23 meV in the ambient air to 40 meV in acetonitrile for (9,7) SWNTs. This linewidth broadening is probably attributed to inhomogeneous broadening due to the fluctuation of local dielectric constant of the environment in the scale of the size of a molecule of the liquids. It should be mentioned that the dielectric constants used in this chapter are macroscopic and static values. In practice, the size of a molecule of the organic solvent is comparable to the size of an exciton, so that the local dielectric constant around the excitons could fluctuate depending on the position and orientation of the organic molecules, which could not follow the dynamic electric field formed by the exciton within the lifetime of the exciton. This results in the dispersion of the energies of many body effects.

3.2 Effect of ambient air and intrinsic transition energies

When measuring PL of free standing SWNTs in a vacuum, the transition energies are 20~40 meV higher than those measured in the ambient air, as shown by the black dots in Fig. 6. Sequential measurements of the PL in the ambient air after the growth of SWNTs show the phenomenon that every E_{ii} shift to lower energies with an incubation time from a few hours to several days. The incubation time to occur the red-shift depends on the diameter of SWNTs, that is, the red-shift occurs from SWNTs with a smaller diameter to those with a larger diameter. This variation of E_{ii} is reversible, namely, E_{ii} returns to its former value when the sample is heated up above 50°C in a vacuum. The shifts of E_{ii} can be attributed to the dielectric screening effect because the way of the shifts is similar to that observed in the liquid immersion experiments.
In the air, the ambient molecules such as H_2O and C_xH_y adsorbed on the surface of SWNTs, and causes the screening of many body interactions. Chiashi et al. have investigated the effect of gas adsorption in detail. (Chiashi et al., 2008) They have shown that the redshift occurs at a gas pressure above a transition pressure, which agrees with Langmuir's adsorption model.
Carrier doping due to oxygen molecules should be discussed as one of the effects of the ambient air because the energies of many body interactions may be modified depending on carrier density. The effect of carrier doping by field-effect doping technique has been studied by PL of the free-standing SWNT placed in a field-effect transistor structure (Ohno et al., 2006c). In addition, the effect of chemical doping with F_4TCNQ (tetrafluorotetracyano-p-quinodimethane), which is a strong p-type dopant for SWNTs (Nosho et al., 2007), also have been studied. Even though the carrier densities doped by these doping techniques were as high as that by the ambient oxygen, the optical transition energies were not

significantly modified by the doping. The doping density would not be high enough to dope carriers in the range of the exciton diameter.
Now, by heating the free standing SWNTs in a vacuum, the adsorbed molecules can be desorbed, and then the *intrinsic* transition energies of SWNTs can be measured without any environmental effects.

3.3 Effect of wrapping with surfactants

When the free-standing SWNTs grown on trenches were immersed in an aqueous solution of SDS (1 wt%), E_{22}-E_{11} plots shifted to the positions as shown by the red stars in Fig. 6. They are almost equal to the data obtained for the SWNTs wrapped by SDS using O'Connell's method as mentioned in section 2.4, which means that the free-standing SWNTs were wrapped by SDS by immersing the solution.
Most E_{11} and E_{22} of SDS-wrapped SWNTs show red-shifts as compared to those of free-standing SWNTs in the air, except for E_{22} of near-zigzag type-II SWNTs, which show blue-shifts. (Ohno et al., 2006b) This behavior is different from the results of the dielectric constant dependence as described above, in which all E_{11} and E_{22} showed red-shifts with increasing the dielectric constant. The positions of the E_{22}-E_{11} plots of SDS-wrapped SWNTs shift so that the $(2n+m)$-family pattern spreads more widely, in addition to the shift due to the dielectric screening effect. This behavior of the energy shifts is similar to stress-induced shift. (Arnold et al., 2004) One plausible explanation for the effect of SDS wrapping is that the SWNT is compressed by the surfactant molecules to the direction of the radius, resulting in the uniaxial strain which modifies the bandgap of the SWNT.

3.4 Effect of substrate

Even though a substrate is one of indispensable parts for device application of SWNTs to support the SWNTs and electrodes, a contact with a substrate seriously affect the optical property of SWNTs. For example, in the case of SWNTs grown on a substrate such as SiO_2, PL is strongly suppressed if the body of the SWNT lies on the substrate. (Lefebvre et al., 2004a, Ohno et al., 2006c) The quenching of PL suggests that the excitons excited in a SWNT recombine by a non-radiative recombination process, probably via interface states between the SWNT and the substrate. The interface states cause also serious problem not only for optical property of SWNTs but also for electrical property of SWNTs, for example, the capture and emission of carriers at the interface states may cause noise in SWNT FETs. (Lin et al., 2007)
Even though PL spectroscopy is not applicable to such SWNTs directly grown on a substrate, photocurrent spectroscopy is useful to study the optical property of the SWNT. (Ohno et al., 2004) Figure 8 shows the photocurrent spectra of two types of transistors, one is a conventional SWNT transistor with a channel lying on a SiO_2/Si substrate, the other is a transistor with a channel of a free-standing SWNT as shown in the inset. The peaks in the spectra are attributed to E_{22} of semiconducting SWNT. In the case of the free standing SWNT, the peak is as sharp as 30 meV in FWHM, which is comparable to the excitation spectrum of the PL of a SWNT. On the other hand, in the case of the SWNT lying on SiO_2, the peak structure is not clear and the FWHM is as broad as 60 meV. The broadening of the spectrum suggests that the energy band of the SWNT is modified inhomogeneously, probably depending on the surface structure of amorphous SiO_2.

Recently, Xie et al. have reported that PL can be observed from SWNTs lying on a SiO_2 surface when the SWNTs are transferred to the other substrate after the growth. (Xie et al., 2007) Even though it is hard to form the interface states at room temperature since both a SWNT and SiO_2 are chemically stable, chemical bonds may be formed at the interface during the growth of SWNTs directly on a substrate due to high growth temperature. Such chemical bonds may act as non-radiative recombination centers. Moreover, they also mentioned that the PL was enhanced when the surface of the substrate is covered with a self-assembled monolayer. It has been explained by carrier transfer to the traps in the SiO_2 film of the substrate.

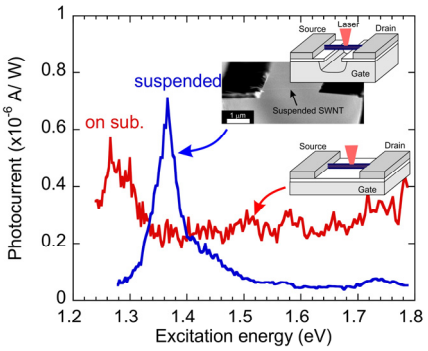

Figure 8 Photocurrent spectra of CNTFETs with a free standing SWNT (blue) and a SWNT contacting with a substrate (red).

4. Summary

In this chapter, we discussed environmental effects on the optical property of SWNTs. Detailed understandings of the environmental effects help us to make the spectroscopic technique a standardized methodology to evaluate the chirality abundance and the quality of SWNTs. It is also interesting to develop sensing tools in nano dimension for bio and medical applications, utilizing the environmental effects.

Acknowledgments

The author thank S. Iwasaki, A. Kobayashi, Y. Murakami, Y. Miyauchi, R. Saito for fruitful collaborations and discussions. This work is partially supported by Grant-in-Aid of MEXT, Japan.

References

Ando, T. (2005) *J. Phys. Soc. Jpn.* Vol. 74, p. 777.
Arnold, K.; Lebedkin, S.; Kiowski, O.; Hennrich, F.; Kappes, M. M. (2004) *Nano Lett.* Vol. 4, p. 2349.

Bachilo, S. M.; Strano, M. S.; Kittrell, C.; Hauge, R. H.; Smalley, R. E.; Weisman, R. B. (2002) *Science* Vol. 298, p. 2361.
Chiashi, S.; Watanabe, S.; Hanashima, T.; Homma, Y. (2008) *Nano Lett.* Vol. 8, p. 3097.
Chou, S. G.; Ribeiro, H. B.; Barros, E. B.; Santos, A. P.; Nezich, D.; Samsonidze, Ge. G.; Fantini, C.; Pimenta, M. A.; Jorio, A.; Filho. F. P.; Dresselhaus, M. S.; Dresselhaus, G.; Saito, R.; Zheng, M.; Onoa, G. B.; Semke, E. D.; Swan, A. K.; Ünlü, M. S.; Goldberg, B. B. (2004) *Chem. Phys. Lett.* Vol. 397, 296.
Duesberg, G. S.; Loa, I.; Burghard, M.; Syassen, K.; Roth, S. (2000) *Phys. Rev. Lett.* Vol. 85, p. 5436.
Fantini, C.; Jorio, A.; Souza, M.; Strano, M. S.; Dresselhaus, M. S.; Pimenta, M. A. (2004) *Phys. Rev. Lett.* Vol. 93, p. 147406.
Finnie, P.; Homma, Y.; Lefebvre J. (2005) *Phys. Rev. Lett.* Vol. 94, p. 247401.
Hagen, A.; Moos, G.; Talalaev, V.; Hertel, T. (2004) *Appl. Phys. A* Vol. 78, p. 1137.
Hertel, T.; Hagen, A.; Talalaev, V.; Arnold, K.; Hennrich, F.; Kappes, M.; Rosenthal, S.; McBride, J. ; Ulbricht, H.; Flahaut, E. (2005) *Nano Lett.* Vol. 5, p. 511.
Hirori, H.; Matsuda, K.; Miyauchi, Y.; Maruyama, S.; Kanemitsu, Y. (2006) *Phys. Rev. Lett.* Vol. 97, p. 257401.
Ichida, M.; Hamanaka, Y.; Kataura, H.; Achiba, Y.; Nakamura, A. (2002) *Physica B* Vol. 323, p. 237.
Iwasaki S.; Ohno, Y.; Murakami, Y.; Kishimoto, S.; Maruyama, S.; Mizutani, T. (2007) arXiv:0704.1018v1 [cond-mat.mtrl-sci]
Jorio, A.; Fantini, C.; Pimenta, M. A.; Capaz, R. B.; Samsonidze, G. G.; Dresselhas, G.; Dresselhaus, M. S.; Jian, J.; Kobayashi, N.; Grüneis, A.; Saito, R., (2005) *Phys. Rev. B* Vol. 71, p. 075401.
Kataura, H.; Kumazawa, Y.; Maniwa, Y.; Umezu, I.; Suzuki, S.; Ohtsuka, Y.; Achiba, Y. (1999) *Synthetic Metals*, Vol. 103, p. 2555.
Lefebvre, J.; Finnie, P.; Homma, Y. (2004) *Phys. Rev. B* Vol. 70, p. 045419.
Lefebvre, J.; Fraser, J. M.; Homma, Y.; Finnie, P. (2004) *Appl. Phys. A* Vol. 78, p. 1107.
Lefebvre, J.; Austing, D. G.; Bond, J.; Finnie, P. (2006) *Nano Lett.* Vol. 6, p. 1603.
Lin, Y.-M.; Tsang, J. C.; Freitag, M.; Avouris, Ph. (2007) *Nanotechnol.* Vol. 18, p. 295202.
Miyauchi, Y.; Chiashi, S.; Murakami, Y.; Hayashida, Y.; Maruyama, S. (2004) *Chem. Phys. Lett.* Vol. 387, p. 198.
Miyauchi, Y.; Saito, R.; Sato, K.; Ohno, Y.; Iwasaki, S.; Mizutani, T.; Jiang, J.; Maruyama, S. (2007) *Chem. Phys. Lett.* Vol. 442, p. 394.
Moore, V. C.; Strano, M. S.; Haroz, E. H.; Hauge, R. H.; Smalley, R. E.; Schmidt, J.; Talmon, Y. (2003) *Nano Lett.* Vol. 3, p. 1379.
Nosho, Y.; Ohno, Y.; Kishimoto, S.; Mizutani, T. (2007) *Nanotechnol.* Vol. 18 p. 415202.
O'Connell, M. J.; Bachilo, S. M.; Huffman, C. B.; Moore, V. C.; Strano, M. S.; Haroz, E. H.; Rialon, K. L.; Boul, P. J.; Noon, W. H.; Kittrell, C.; Ma, J.; Hauge, R. H.; Weisman, R. B.; Smalley, R. E. (2002) *Science* Vol. 297, p. 593.
Ohno, Y.; Kishimoto, S.; Mizutani, T.; Okazaki, T.; Shinohara, H. (2004) *Appl. Phys. Lett.* 84, 1368.
Ohno, Y.; Shimada, T.; Kishimoto, S.; Maruyama, S.; Mizutani, T. (2006) *J. Physics: Conf. Series* Vol. 38, p. 5.
Ohno, Y.; Iwasaki, S.; Murakami, Y.; Kishimoto, S.; Maruyama, S.; Mizutani, T. (2006) *Phys. Rev. B* Vol. 73, p. 235427.

Ohno, Y.; Kishimoto, S.; Mizutani, T. (2006) *Nanotechnol.* Vol. 17, p. 549.
Ohno, Y.; Iwasaki, S.; Murakami, Y.; Kishimoto, S.; Maruyama, S.; Mizutani, T. (2007) *phys. stat. sol (b)* Vol. 244, p. 4002,
Okazaki, T.; Saito, T.; Matsuura, K.; Ohshima, S.; Yumura, M.; Oyama, Y.; Saito, R.; Iijima, S. (2006) *Chem. Phys. Lett.* 420, 286.
Ostojic, G. N.; Zaric, S.; Kono, J.; Strano, M. S.; Moore, V. C.; Hauge, R. H.; Smalley, R. E. (2004) *Phys. Rev. Lett.* Vol. 92, p. 117402.
Oyama, Y.; Saito, R.; Sato, K.; Jiang, J.; Samsonidze, G. G.; Grüneis, A.; Miyauchi, Y.; Maruyama, S.; Jorio, A.; Dresselhaus, G.; Dresselhaus, M. S. (2006) *Carbon* Vol. 44, p. 873.
Perebeinos, V.; Tersoff, J.; Avouris, Ph. (2004) *Phys. Rev. Lett.* Vol. 2, p. 257402.
Saito, R.; Dresselhaus, G.; Dresselhaus, M. S. (1998) *Physical Properties of Carbon Nanotube*, Imperial College Press, London.
Saito, R.; Dresselhaus G.; Dresselhaus, M. S. (2000) *Phys. Rev. B* Vol. 61, p. 2981.
Spataru, C. D.; I-Beigi, S.; Capaz, R. B.; Louie, S. G. (2005) *Phys. Rev. Lett.* Vol. 95, p. 247402.
Wang, F.; Dukovic, G.; Brus, L. E.; Heinz, T. F. (2004) *Phys. Rev. Lett.* Vol. 92, p. 177401.
Wang, F.; Dukovic, G.; Brus, L. E.; Heinz, T. F. (2005) *Science* Vol. 308, p. 838.
Xie, L.; Liu, C.; Zhang, J.; Zhang, Y.; Jiao, L.; Jiang, L.; Dai, L.; Liu, Z. (2007) *J. Am. Chem. Soc.* Vol. 129, p. 12382.

Footnote1: Note that while the dielectric constants for dc filed are used in this chapter, they are dependent on the frequency of field. At the frequency corresponding to the exciton lifetime, dielectric constant should become close to unity. Although the exact values of ac dielectric constants of these liquids have not been known, they could be related to the dc dielectric constants.